Magnetoresistance in One- and Two-Dimensional Lateral Surface Superlattices

D. Weiss

Max-Planck-Institut für Festkörperforschung, Heisenbergstr. 1,
D-7000 Stuttgart 80, Fed. Rep. of Germany

The low temperature magnetoresistance of a high mobility two-dimensional electron gas is dominated by Shubnikov-de Haas oscillations, reflecting the discrete nature of the electron energy spectrum. When a weak one- or two-dimensional periodic potential is superimposed on the two-dimensional electron gas, a novel type of oscillation occurs which reflects the commensurability of the relevant lengths in these systems – the cyclotron orbit diameter at the Fermi energy and the period a of the periodic potential. In addition the electron mean free path l_e also plays a role since the effect is observable only in mesoscopic systems where l_e is significantly longer than the period a of the potential. The essential aspects of these novel commensurability oscillations are sketched. The observed positive magnetoresistance at very low magnetic fields is discussed in terms of magnetic breakdown.

1. Introduction

At low temperatures the magnetoresistance of a degenerate two-dimensional electron gas (2-DEG) exhibits the well known Shubnikov-de Haas (SdH) oscillations reflecting the discrete nature of the degenerate Landau energy spectrum [1]. Using modern lithographic techniques [2] one can superimpose a periodic potential on such a 2-DEG. Now the conduction electrons have to move under the combined influence of a one- or two-dimensional periodic potential and a perpendicular magnetic field B. Such systems have recently attracted some interest since the superimposed periodic potential leads to a novel type of magnetoresistance oscillation periodic in 1/B as long as the period of the modulation is small compared to the mean free path of the electrons [3]. The periodicity of these oscillations is governed by an interesting commensurability problem owing to the presence of two length scales , the period a of the potential and the cyclotron radius R_C at the Fermi energy [3,4]. We have used the persistent photoconductivity effect (PPC) to create one- and two-dimensional periodic potentials in the submicrometer range. A spatially modulated photon flux results in a spatially modulated positive background charge in the Si-doped AlGaAs layer which in turn leads to a modulation in the carrier density. In our measurements a holographic illumination of the heterostructure at liquid helium temperatures is used to produce a periodic potential with a period on the order of the wavelength of the interfering beams, a method first used by Tsubaki et al. [5]. The potential modulation obtained by this technique is on the order of 1 meV where the Fermi energy E_F in our samples is typically 10 meV. Assuming a 1D-periodic potential in x-direction the energy spectrum and the contours of constant energy at the Fermi energy E_F are sketched in Fig.1. Without periodic modulation one obtains the well known parabolic energy dispersion characteristic for a 2-DEG and the contour of constant energy at E_F is a circle with radius k_F. Switching on a weak magnetic field would force the electrons around this Fermi circle corresponding also to a circular motion in real space. The effect of a superimposed periodic potential with period a is that it opens up gaps at the new Brillouin zone boundaries at multiples of $\pm\pi/a$ as is sketched in Fig.1. The existence of gaps at the Bragg planes lead to open orbits in k_x-direction (dashed-dotted line on the right hand side in Fig.1) connected to an electron motion in y-direction in real space. This additional conductivity in y-direction is known to give a positive magnetoresistance ρ_{xx} [6] in x-direction. Increasing the magnetic field increases the probability for an electron

Springer Series in Solid-State Sciences, Vol. 97
Localization and Confinement of Electrons in Semiconductors
Editors: F. Kuchar · H. Heinrich · G. Bauer

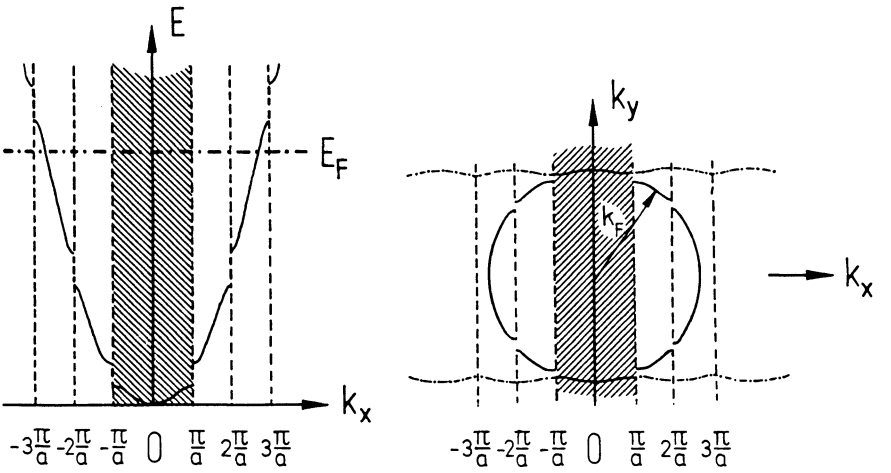

Figure 1: Energy dispersion and contours of constant energy for a weak 1D-periodic potential superimposed on a 2-DEG. The new reciprocal lattice vector is $2\pi/a$ where a is the superlattice period. The first Brillouin zone is hatched. The existence of open orbits at sufficiently low magnetic fields (dashed-dotted line on the right hand side) modifies the low field magnetoresistance.

to tunnel through the classically forbidden region and performing now a circular motion. This effect is known as magnetic breakdown [7]. Under this condition the positive magnetoresistance saturates since the electrons now behave as in a homogeneous 2-DEG. Since we have a weak periodic potential only the gaps between the lowest bands will be significant [8]. For a typical period of $300nm$ and a carrier density $N_S = 2 \cdot 10^{11} cm^{-2}$ we note that we have about 10 bands occupied corresponding to 20 Bragg planes intersecting the original Fermi circle. Therefore we do not expect a significant influence of the periodic potential on the transport properties at zero magnetic field since the Fermi energy is located high in the bandstructure where the dispersion is almost that of a free 2-DEG. The situation changes, however, when a magnetic field is switched on. This will be shown in the next section, where the experiments displaying the novel magnetoresistance oscillations are briefly reviewed.

2. Magnetoresistance Oscillations

The experiments were carried out using conventional AlGaAs-GaAs heterostructures grown by molecular beam epitaxy with carrier densities between $1.5 \cdot 10^{11} \mathrm{cm}^{-2}$ and $4.3 \cdot 10^{11}$ cm^{-2} and low temperature mobilities ranging from $0.23 \cdot 10^6 \mathrm{cm}^2/\mathrm{Vs}$ to $1 \cdot 10^6 \mathrm{cm}^2/\mathrm{Vs}$. Illumination of the samples increases both the carrier density and the mobility at low temperatures. We have chosen an L-shaped geometry to investigate the magnetotransport properties parallel and perpendicular to the interference fringes. Some of the samples investigated have an evaporated semi-transparent NiCr front gate. A sketch of the experiment exploiting the persistent photoconductivity to periodically modulate the positive background charge in the AlGaAs-layer is shown in Fig.2a and 2b. We used either a HeNe laser (λ = 633nm) or an Argon-Ion laser (λ = 488nm). The expanded laser beam entered the sampleholder through a quartz window and a shutter. Two mirrors mounted close to the sample were used to create two interfering plane waves. The advantage of this kind of 'microstructure engineering' is its simplicity and the achieved high mobility of the microstructured sample due to the absence of defects introduced by the usual pattern transfer techniques [2].

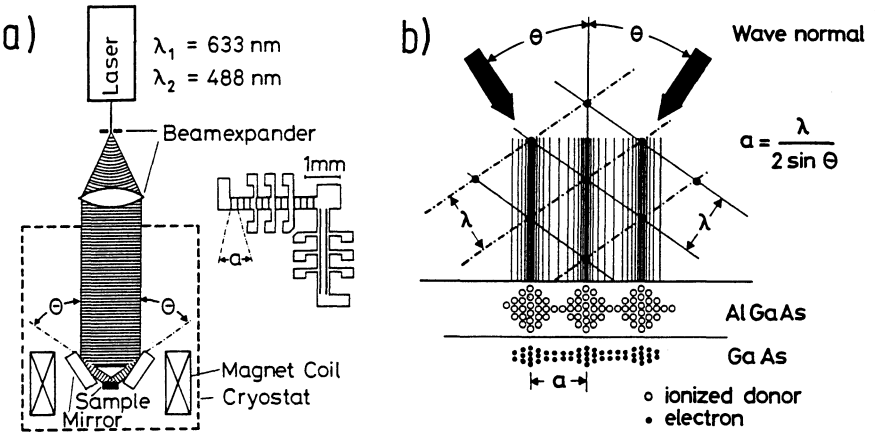

Figure 2: Schematic experimental set up (left hand side) and top view of the L shaped sample geometry where the interference pattern is sketched (a). Sketch of the spatial modulation of the concentration of ionized donors in the AlGaAs layer and of electrons in the 2-DEG produced by holographic illumination using two interfering laser beams with wavelength λ. The interference pattern created is shown schematically (b).

The result of standard magnetoresistance measurements carried out perpendicular ($\rho_\perp = \rho_{xx}$) and parallel ($\rho_{||} = \rho_{yy}$) to the periodic modulation is shown in Fig.3. In addition to the usual Shubnikov-de Haas oscillations appearing at about 0.5T additional oscillations become visible at even lower magnetic fields. While pronounced oscillations of this new type dominate $\rho_\perp$ at low magnetic fields, weaker oscillations with a phase shift of 180^0 relative to the $\rho_\perp$ data are visible in the $\rho_{||}$ measurements. No additional structure appears in the Hall resistance. The novel oscillations are, analogous to SdH oscillations, periodic in 1/B as is displayed in the inset of Fig.3. The periodicity is given by the commensurability condition

$$2R_c = (\lambda - \frac{1}{4})a, \qquad \lambda = 1, 2, 3, ..., \tag{1}$$

between the cyclotron diameter at the Fermi level, $2R_c = 2v_F/\omega_c = 2l^2k_F$, and the period a of the modulation. Here $k_F = \sqrt{2\pi N_s}$ is the Fermi wavenumber, $l = \sqrt{\hbar/eB}$ the magnetic length, and $\omega_c = \hbar/m^*l^2$ the cyclotron frequency with the effective mass $m^* = 0.067m_0$ of GaAs. For magnetic field values satisfying Eq.(1) minima are observed in $\rho_\perp$. The periodicity $\Delta(1/B)$ can easily be deduced from Eq.(1)

$$\Delta\frac{1}{B} = e\frac{a}{2\hbar k_F} \quad . \tag{2}$$

The validity of Eq.(1) has been confirmed by performing these experiments on different samples, by changing the carrier density with an applied gate voltage, and by using two laser wavelengths in order to vary the period a [3]. To resolve an oscillation an elastic mean free path l_e at least as long as the perimeter of the cyclotron orbit is required. This agrees with our finding that the number of oscillation periods resolved depends on the mobility of the sample: the higher the mobility the more oscillations are observable since the electrons can traverse more periods of the potential ballistically. Consistent experimental results have been obtained by Winkler et al. [9] and Alves et al. [10] using conventionally microstructured samples. The key for the explanation of this novel oscillatory behaviour of ρ_{xx} and ρ_{yy} in such periodically modulated 2-DEG's is a modification of the Landau level spectrum discussed in the next section.

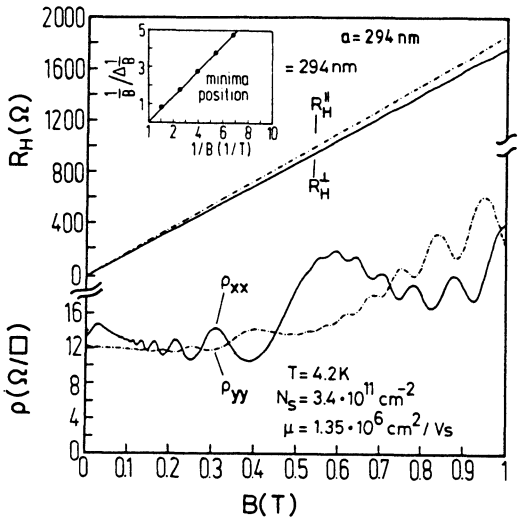

Figure 3: Magnetoresistivity ρ and Hall resistance R_H parallel and perpendicular to the interference fringes. The positions of the minima of $\rho_\perp$ are plotted in the inset demonstrating the 1/B periodicity of the novel oscillations.

3. Origin of the Oscillations

The common origin of both types of oscillations observed is due to a modification of the Landau level (LL) energy spectrum. This has been pointed out by Gerhardts et al. [4] and Winkler et al. [9] who contributed the $\rho_\perp$ oscillations to an additional band conductivity discussed in section 3.2. However, there are other models explaining the $\rho_\perp$ oscillations. Beenakker [11] noticed that these oscillations can be attributed to a guiding center drift resonance. He showed for high temperatures that it is not necessary to start from the LL energy spectrum and to treat the problem quantum-mechanically. In this limit the oscillations in $\rho_\perp$ can be explained semiclassically. Quite recently Streda and MacDonald [12] explained the oscillations by an oscillating probability for magnetic breakdown. However, all the theories above cannot explain the oscillations in $\rho_{||}$. One has to go beyond the constant scattering time approximation as has been pointed out first by Gerhardts [8].

3.1 Landau Levels in a 1D-Periodic Potential

The energy spectrum of electrons subjected to both a magnetic field and a periodic one-dimensional potential has been calculated by several authors [13,14,15] using first order perturbation theory. Starting point is a Hamiltonian of the form

$$H = \frac{1}{2m^*}\left[-\hbar^2\frac{\partial^2}{\partial x^2} + \left(\frac{\hbar}{i}\frac{\partial}{\partial y} + \frac{e}{c}Bx\right)^2\right] + V_0 cos(Kx) \qquad (3)$$

containing a periodic potential in x-direction $V(x) = V_0 cos(Kx)$ with period $a = 2\pi/K$. The energy spectrum can be taken in first order perturbation theory in V and is given by

$$E_n(x_0) \approx (n + \frac{1}{2})\hbar\omega_c + \langle nx_0 \mid V(x) \mid nx_0\rangle. \qquad (4)$$

The right hand side matrix element (containing the wavefunctions $\mid nx_0\rangle$ of the homogeneous 2-DEG) can be regarded as effective potential acting on an electron averaged over the spatial extent of the wavefunction $\mid nx_0\rangle$ given by $2l\sqrt{2n+1}$ which is equal to the classical cyclotron diameter $2R_c$ for high quantum numbers n. Two extremal situations can be considered. Assuming, for sake of simplicity, a stepfunction-like wavefunction, the matrix element $\langle nx_0 \mid V(x) \mid nx_0\rangle$ at the Fermi energy vanishes if the cyclotron diameter equals an integer of the period a leading to a flat Landau band, independent

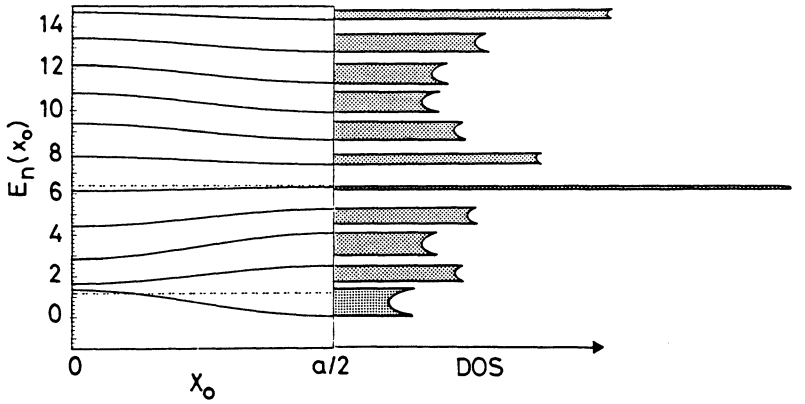

Figure 4: Calculated energy spectrum (in meV, first order perturbation theory) for B=0.8T, $V_0 = 1.5meV$ and a=100nm. The corresponding DOS is sketched. The dashed lines correspond to the flat band situation determined by Eq.(1).

of the center coordinate x_0. On the other hand, a maximum of the matrix element is expected for a cyclotron diameter equal to an odd integer of half the period a leading to Landau bands with strong curvature with respect to x_0. More precisely, the matrix element $\langle nx_0 \mid V(x) \mid nx_0 \rangle$ can be calculated analytically giving

$$E_n(x_0) \approx (n + \frac{1}{2})\hbar\omega_c + U_n cosKx_0 \tag{5}$$

with $U_n = V_0 \exp(-\frac{1}{2}X)L_n(X)$ where $X = \frac{1}{2}K^2l^2$ and $L_n(X)$ stands for the n-th Laguerre polynomial. $L_n(X)$ is an oscillating function of both its index n and its argument X where the flat band situation is given by $L_n(X) = 0$. This flat band condition can be expressed in terms of the cyclotron radius R_c and is given by Eq.(1) [4]. A typical energy spectrum – calculated in first order perturbation theory is plotted in Fig.4. The corresponding DOS is sketched on the right hand side in Fig.4. Note the double peak structure of the DOS at the band edges which one typically expects for a 1D bandstructure due to the van Hove singularities. These singularities have been recently investigated experimentally [16].

The existence of the shape of the DOS sketched in Fig.4 can be directly proven by magnetocapacitance experiments. The magnetocapacitance C(B) – measured between the semi-transparent top gate and the 2-DEG – depends not only on the thickness of the dielectric layers but also on the thermodynamic DOS [17,18]. When the Fermi energy is located in a LL (maximum DOS) the capacitance displays a maximum; a minimum in C(B) is observed when E_F is between two LL's (minimum DOS). The height of these magnetocapacitance oscillations is directly connected to the thermodynamic DOS and gives therefore information about the LL-width Γ. This has been used previously in homogeneous systems to investigate systematically the LL-width Γ as a function of the electron mobility in such samples [19]. In Fig.5 the magnetocapacitance after an initial holographic illumination (a) is compared with the capacitance measured after an additional illumination which essentially smears out the periodic modulation (b) [20]. In contrast to Fig.5b, where the magnetocapacitance behaves as usually observed in a 2-DEG, the capacitance oscillations in Fig.5a display a pronounced modulation of both the minima and maxima which is easily explained from the energy spectrum plotted in Fig.4. At about 0.69 T (marked by an arrow) the cyclotron diameter at the Fermi energy equals three quarter of the period a and corresponds to the last flat band situation ($\lambda = 1$). Therefore, the magnetocapacitance values near 0.69 T are approximately equal in Fig.5a and Fig.5b. If now the magnetic field is increased, modulation broadened Landau bands are swept through the Fermi level, and cause the nonmonotonic behaviour visible in Fig.5a. At

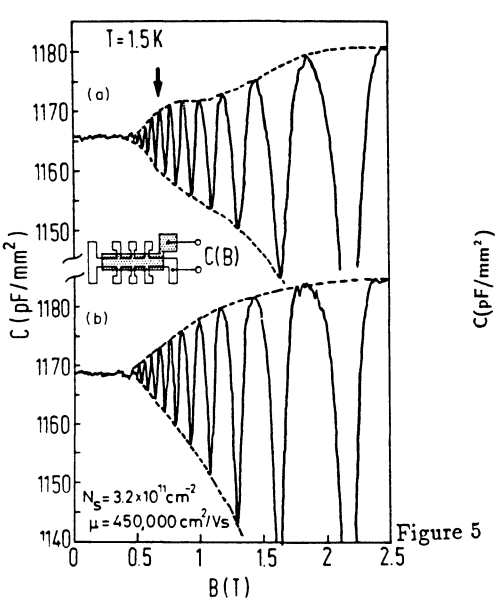

Figure 5

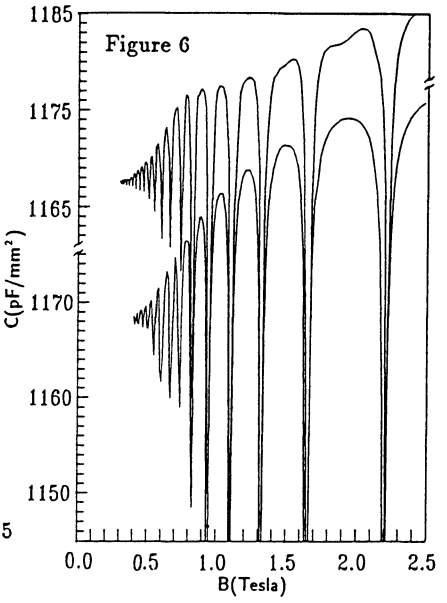

Figure 5: Measured magnetocapacitance (a) of a modulated sample (a=365nm) compared to the capacitance of an essentially unmodulated sample (b). The arrow corresponds to the magnetic field value fulfilling Eq.(1) for $\lambda = 1$.

Figure 6: Calculated magnetocapacitance versus magnetic field for $N_S = 3.2 \cdot 10^{11} cm^{-2}$ and $a = 365nm$. The upper curve is for $V_0 = 0.7meV$, and the lower one for the weak modulation $V_0 = 0.1meV$.

higher magnetic fields the modulation broadening saturates and the usual LL degeneracy again raises the DOS in a LL with increasing field. The discussion of the magnetocapacitance up to now uses qualitative arguments rather than quantitative ones. In order to check the magnetocapacitance data theoretically, microscopic calculations of the DOS based on a generalization of the well known selfconsistent Born approximation [21] have been performed by Zhang [20]. Once the DOS is calculated the data can be easily converted into magnetocapacitance data. Calculating the magnetocapacitance for a modulation amplitude $V_0 = 0.7meV$ (Fig.6) reproduces the experimentally observed modulation of the envelope of the capacitance maxima (Fig.5a). A weaker amplitude of the periodic potential $V_0 = 0.1meV$ leads to the behaviour of the envelope usually observed in homogeneous 2-DEG's. In Fig.6 an intrinsic linewidth broadening $\Gamma = 0.3meV$ has been assumed. The modified energy spectrum which has been proven experimentally in this section is the key for the explanation of the periodic potential induced oscillations given in the next section.

3.2 Oscillations in $\rho_\perp$: Additional Bandconductivity

The theory presented here follows closely the calculations of Gerhardts et al. [4] for a cosine modulation in x-direction. The oscillations in $\rho_\perp$ ($= \rho_{xx}$) can be understood within a simple damping theory which means that electron scattering is described by a constant relaxation time τ. The k_y dispersion of the Landau energy spectrum leads to an additional contribution to the conductivity σ_{yy} which is within the framework of Kubo's formula (see e.g. Ref.[22]) given by

$$\Delta\sigma_{yy} = \frac{2e^2\hbar}{2\pi l^2} \int_0^a \frac{dx_0}{a} \sum_n \left(-\frac{1}{\gamma} \frac{df}{dE}(E_n(x_0)) \mid \langle nx_0 \mid v_y \mid nx_0 \rangle \mid^2 \right) \qquad (6)$$

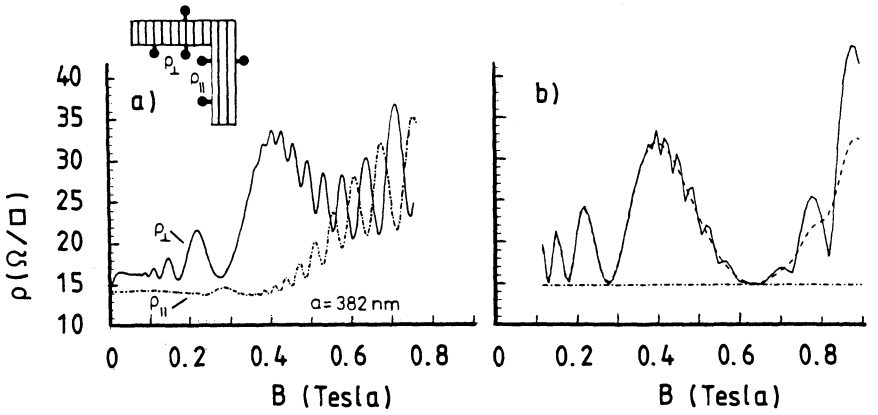

Figure 7: Magnetoresistivities for current perpendicular and parallel to the interference fringes for a sample with $N_S = 3.16 \cdot 10^{11} cm^{-2}$, and $\mu = 1.3 \cdot 10^6 cm^2/Vs$ (a) measured at temperature $T = 2.2K$; (b) calculated for $T = 2.2K$ (solid line) and for $4.2K$ (dashed line) [4].

where $\gamma = \hbar/\tau$, f is the Fermi function, $\mid nx_0\rangle$ are the eigenstates of Eq.(3) and v_y is the velocity operator in y direction. These eigenstates carry current in the y direction

$$\langle nx_0 \mid v_y \mid nx_0\rangle = -\frac{1}{m^*\omega_c}\frac{dE_n}{dx_0} = \frac{1}{\hbar}\frac{dE_n}{dk_y} \tag{7}$$

but not in x-direction,

$$\langle nx_0 \mid v_x \mid nx_0\rangle = 0, \tag{8}$$

which is the reason for the anisotropic behaviour of σ_{xx} (corresponding to ρ_{yy}) and σ_{yy} (corresponding to ρ_{xx}). In Eq.(7) the modified energy spectrum comes into play. The matrix element $\langle x_0 n \mid v_y \mid x_0 n\rangle$ vanishes always then when flat Landau bands (see e.g. Fig.4) are located at the Fermi energy, and $\Delta\sigma_{yy} = 0$. Consequently also $\Delta\rho_{xx}$ – the extra contribution to the resistivity ρ_{xx} – vanishes since $\Delta\rho_{xx} \approx \Delta\sigma_{yy}/\sigma_{xy}^2$ if $\omega_c\tau > 1$. On the other hand dE_n/dx_0 displays a maximum value when the Fermi energy is located within the Landau band with the strongest dispersion and therefore $\Delta\sigma_{yy}$ ($\Delta\rho_{xx}$) is at maximum. A calculation based on the evaluation of Eq.6 which is compared to experimental magnetoresistivity data is shown in Fig. 7. Assuming a modulation potential of 0.3 meV in the calculations reproduces nicely the oscillations of ρ_{xx} (solid lines in Fig.7). Note that the weak temperature dependence of the commensurability oscillations in ρ_{xx} is given correctly by the calculation in agreement with the experiment [3]. The temperature dependence of these oscillations is much weaker than that of SdH oscillations, since the relevant energy is the distance between flat bands, which is much larger than the mean distance between adjacent bands. In the high temperature limit ($\hbar\omega_c < kT$) and for high quantum numbers n the expression for the additional conductivity becomes much simpler [9] and can be expressed making use of the fact that $\Delta\rho_{xx} \approx \sigma_{yy}/\sigma_{xy}^2$:

$$\Delta\rho_{xx} \approx \frac{1}{2\pi\hbar}\frac{V_0^2}{\gamma\hbar\omega_c}\frac{4}{ak_F}\frac{B^2}{N_s^2}\ cos^2\ (2\pi\frac{R_c}{a} - \frac{\pi}{4}). \tag{9}$$

Equation (9) may be used to estimate from the amplitudes $\Delta\rho_{xx}^{max}$ of the commensurability oscillations the amplitude V_0 of the superimposed periodic potential. From the maximum of ρ_{xx} at 0.41T (Fig.7a) one estimates $V_0 = 0.28meV$ in good agreement with the calculation in Fig.7b.

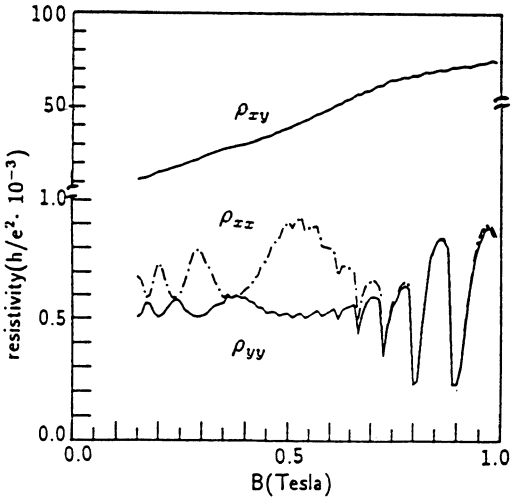

Figure 8: Calculated magnetoresistivity and Hall resistance for T=4.2K, and a=294nm. The oscillations in ρ_{yy} are due to a DOS dependent scattering rate while the oscillations in ρ_{xx} are dominated by the additional bandconductivity (Gerhardts and Zhang [24]).

While the low field oscillations of ρ_{xx} are nicely reproduced by the calculation, the calculated ρ_{yy}-data (dashed-dotted line in Fig.7b) display simply the magnetic field independent Drude result in contrast to the experiment which shows maxima when the Landau bands are flat (DOS maximum at E_F). This is not too surprising since one cannot describe the usual SdH oscillations of a homogeneous 2-DEG within the constant relaxation time approximation; one ends up with the simple Drude result. The same result has been obtained by Beenakker using his semiclassical model [11].

3.3 Oscillations in $\rho_{||}$: Oscillating Scattering Rate

The results in the previous section have been obtained using the constant scattering time approximation which, however, has no justification. For a homogeneous electron gas in a quantizing magnetic field e.g. it is well known that the scattering time itself depends on the DOS [21]. In order to understand the experimentally observed $\rho_{yy}(=\rho_{||})$ oscillations one has to go beyond this approximation – in analogy to the description of the SdH oscillations – and consider a density-of-state-dependent scattering rate. In the calculations one has to go through the formalism of the selfconsistent Born approximation [21] using the solutions of Eq.2. A detailed description of this theory has been given by Zhang and Gerhardts [23]. In analogy to the theory of SdH oscillations they find that

$$\sigma_{xx} \propto D_T^2(\mu) = \int dE \frac{df(E-\mu)}{d\mu} D(E)^2 \tag{10}$$

where $D_T^2(\mu)$ is the thermal average of the square of the DOS. It should be emphasized that even for $kT \approx \hbar\omega_c$ where the individual LL's are no longer resolved in ρ_{yy}, $D_T^2(\mu)$ oscillates, reflecting the oscillating DOS sketched in Fig.4. Consequently one can observe low field oscillations in ρ_{yy} even when in this magnetic field range no SdH oscillations can be resolved. From Eq.10 follows that the weak antiphase oscillations in ρ_{yy} are in phase with the density of states oscillations and maxima in ρ_{yy} are always observed when the DOS at the Fermi-energy is at maximum, in contrast to ρ_{xx} which displays minima when the Landau bands are flat since $dE_n/dx_0 = 0$. Calculated curves of ρ_{xx} and ρ_{yy} taken from Gerhardts and Zhang [24] are shown in Fig.8 demonstrating this behaviour in agreement with the experiment (Fig.3). Recent calculations by Vasilopoulos and Peeters [25] show similar results but with much smaller amplitude of the ρ_{yy} oscillations.

4. Positive Low Field Magnetoresistance and Magnetic Breakdown

The low field oscillations in $\rho_\perp$ are accompanied by a positive low field magnetoresistance which saturates below 0.2T. This positive magnetoresistance is absent in $\rho_{||}$ as is displayed in Fig.3. Applying a negative gate voltage on the semi-transparent top gate one can increase the built in periodic modulation amplitude V_0 [16] which results in turn in an increased positive magnetoresistance step shown in Fig.9. Such a behaviour would be expected for magnetic breakdown, mentioned in the introduction. Open orbits in k_x direction (see Fig.1b or inset Fig.10) give an additional contribution to σ_{yy} and lead to a positive magnetoresistance in ρ_{xx} [6] as long as the electrons can move in open orbits. The probability p for an electron to tunnel from an open orbit (a) to a circular orbit (b) in Fig.10 is given in the literature by $p = exp(-B_0/B)$ with the magnetic breakdown field B_0:

$$B_0 = \frac{\pi m^* E_g^2}{4e\hbar E_F sin2\Theta} \tag{11}$$

where E_g is the energy gap at the Brillouin zone boundary and Θ the angle defined by $cos\Theta = \pi/ak_F$ [26]. For sufficiently weak periodic potentials we may assume – following Streda and MacDonald [12] – that gaps $E_g \approx V_0$ exist only at the boundary of the *first* Brillouin zone (assuming more a situation sketched in the inset of Fig.10 rather than in Fig.1b). Using Eq.(9) we can extract V_0 from the low field ρ_{xx} oscillations in Fig.9 and compare the calculated B_0 values with those taken from the experiment (the magnetic field where the positive magnetoresistance saturates). The comparison is plotted in Fig.10. The calculated B_0 values are not in perfect agreement with the experimental ones. For higher modulation amplitudes V_0, Eq.(11) overestimates the breakdown field B_0. One should bear in mind, however, that we do not take into account finite temperature effects and the higher gaps sketched in Fig.1b.

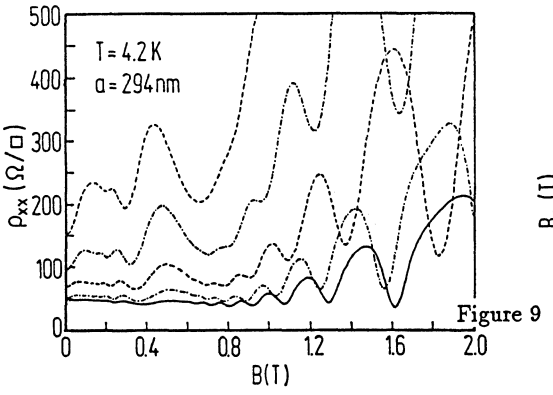

Figure 9

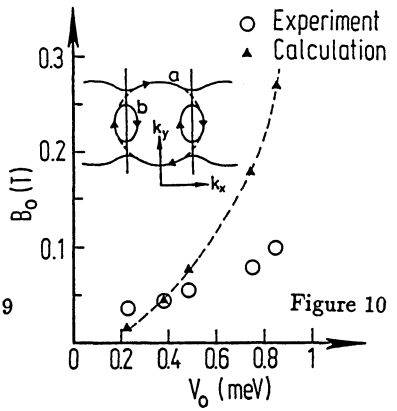

Figure 10

Figure 9: ρ_{xx} for different gate voltages (0mV, -100mV, -200mV, -300mV, -400mV from bottom to top). With increasing negative bias, both the amplitude of the low field oscillations and the magnetic field value where the positive magnetoresistance disappears (taken as B_0) increase

Figure 10: Comparison of calculated (Eq.(11)) and measured (Fig.9) breakdown fields B_0. The inset shows the contours of constant energy at E_F for a weakly modulated 2-DEG in the extended zone scheme.

5. Magnetoresistance in a Two-Dimensional Periodic Potential

In this last section some preliminary results of low field magnetotransport experiments in a two-dimensional periodic potential are presented. In such a potential grid the commensurability problem becomes more severe as compared to the 2-D case and results in a complicated energy spectrum [27]. In a weak 2D-periodic potential the LL spectrum depends on the flux $\Phi = Ba^2$ penetrating one unit cell. If $\Phi/\Phi_0 = q/p$ where Φ_0 is the flux quantum and p/q is a rational number, the 2D-periodic potential splits one LL into q subbands separated by gaps (see e.g. [28]). The LL width ,on the other hand, is modulated by Laguerre polynominals very similar to the 1D case (Eq.(4)), so that the flat band condition for 1D-and 2D-periodic potentials is the same [29]. The two-dimensional periodic potential ($V_0 \ll E_F$) with $a = 365nm$ is created by successively illuminating holographically a high mobility heterostructure ($\mu = 1.2 \cdot 10^6 cm^2/Vs$). Holographic illumination of type (a) in Fig.11 produces additional oscillations in the magnetoresistance due to an additional bandconductivity (dashed-dotted line in Fig.11). An additional holographic illumination where the sample has been rotated by 90° results then in a grid potential sketched in Fig.11 (c). The magnetoresistance obtained under such conditions (solid line in Fig.11) displays a weak oscillating behaviour also corresponding to the commensurability condition Eq.(1), with maxima where ρ_{xx} -measured for situation (a)- shows minima. If one starts with an illumination of type (b) followed by (a) one ends up with the same result. The result obtained for the magnetoresistance in a two-dimensional periodic potential is therefore very close to the result one gets when the current flows parallel to the potential grating, discussed as additional oscillations in ρ_{yy} above (see section 3.3). Therefore one can conclude that the 2D-periodic potential destroys the bandconductivity oscillations triggered by $\langle nx_0|v_y|nx_0\rangle \propto dE_n/dk_y$ for the 1D case. If the collision broadening for the 2D case is small compared to the gaps between the LL subbands the corresponding matrix elements are significantly reduced so suppressing the bandconductivity contribution [29]. Since this seems to be the case in our experiments we can only observe the scattering rate oscillations displaying maxima when the flat band condition Eq.(1) is fulfilled.

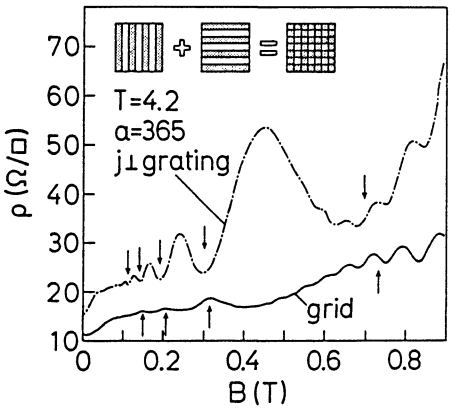

Figure 11: Magnetoresistance in a grating (j ⊥ grating) and grid. The creation of the holographically defined pattern is shown schematically. The arrows correspond to Eq.(1).

I would like to thank K. von Klitzing , R. R. Gerhardts, C. Zhang, U. Wulf, G. Müller, and D. Heitmann for valuable discussions and I am grateful to K. Ploog and G. Weimann for providing me with high quality samples.

6. References

[1] L. Shubnikov, W. J. de Haas, *Leiden Commun.* **207a, 207c, 207d, 210a** (1930)

[2] For recent work in this field see *Physics and Technology of Submicron Structures*, ed. by H. Heinrich, G. Bauer, and F. Kuchar, Springer Series Solid-State Sciences **83**, (1988)

[3] D. Weiss, K. v. Klitzing, K. Ploog, G. Weimann *Europhys. Lett.* **8**, 179 (1989); also in *The Application of High Magnetic Fields in Semiconductor Physics*, ed. G. Landwehr, Springer Series in Solid-State Sciences **87** , 357 (1989)

[4] R. R. Gerhardts, D. Weiss, K. v. Klitzing; *Phys. Rev. Lett.* **62**, 1173 (1989)

[5] K. Tsubaki, H. Sakaki, J. Yoshino, Y. Sekiguchi, *Appl. Phys. Lett.* **45**, 663 (1984)

[6] C. Kittel; Quantum Theory of Solids, Wiley, New York, (1967)

[7] M. H. Cohen, L. M. Falicov; *Phys. Rev. Lett.* **7**, 231, (1961)

[8] R.R.Gerhardts in "Science and Engineering of 1- and 0-Dimensional Semicondcutors", edited by S.P. Beaumont and C.M. Sotomayor Torres (Plenum, London), Proc. NATO ARW, 29 March - 1 April 1989, Cadiz, Spain, to be published

[9] R. W. Winkler, J. P. Kotthaus, K. Ploog; *Phys. Rev. Lett.* **62**, 1177 (1989)

[10] E. S. Alves, P. H. Beton, M. Henini, L. Eaves P. C. Main, O. H. Hughes, G. A. Toombs, S. P. Beaumont, C. D. W. Wilkinson; *J. Phys.: Condens. Matter* **1**, 8257, (1989)

[11] C.W.J. Beenakker; *Phys. Rev. Lett.* **62** , 2020, (1989)

[12] P. Streda, A. H. MacDonald; preprint

[13] G. R. Aizin, V. A. Volkov; Sov. Phys. JETP **60**, 844 (1984) [Zh. Eksp. Teor. Fiz **87**, 1469 (1984)]

[14] H. J. Kelly; *J. Phys. C* **18**, 6341 (1985)

[15] A. V. Chaplik; *Solid State Commun.* **53**, 539, (1985)

[16] D. Weiss, K. von Klitzing, K. Ploog, G. Weimann; *Surface Science* **229**, 88 (1990)

[17] T. P. Smith, B. B. Goldberg, P. J. Stiles, M. Heiblum, *Phys. Rev.* **B32**, 2696 (1985)

[18] V. Mosser, D. Weiss, K. v. Klitzing, K. Ploog, G. Weimann, *Solid State Commun.* **58**, 5 (1986)

[19] D. Weiss, K. v. Klitzing in *High Magnetic Fields in Semiconductor Physics*, ed. G. Landwehr, Springer Series in Solid-State Sciences **71**, 57 (1987)

[20] D. Weiss, C. Zhang, R. R. Gerhardts, K. von Klitzing, G. Weimann; *Phys. Rev.* **B39**, 13030 (1989)

[21] T. Ando, Y. Uemura, *J. Phys. Soc. Jpn.* **36**, 959 (1974); R. R. Gerhardts, *Z. Physik* **B21**, 285 (1975)

[22] R. Kubo, S. J. Miyake, N. Hashitsume; *Solid State Physics* **17**, 239 (1965)

[23] C. Zhang, R. R. Gerhardts; submitted to Phys. Rev. B

[24] R. R. Gerhardts, C. Zhang; *Surface Science* **229**, 92 (1990)

[25] P. Vasilopoulos, F. M. Peeters *Phys. Rev. Lett.* **63**, 2120 (1989)

[26] E. I. Blount;*Phys. Rev.* **126**, 1636 (1962); A. B. Pippard; *Proc. Roy. Soc. (London) A*, **270**, 1 (1962); J. R. Reitz; *J. Phys. Chem. Solids* **25**, 53 (1964)

[27] D. R. Hofstadter; *Phys. Rev.* **B14**, 2239 (1976)

[28] D. J. Thouless; in *The Quantum Hall Effect* ed. by R. E. Prange and S. M. Girvin, Springer (1987)

[29] R. R. Gerhardts, D. Weiss, U. Wulf; unpublished